Energetic Cost and Structural Consequences of Burying a Hydroxyl Group within the Core of a Protein Determined from Ala → Ser and Val → Thr Substitutions in T4 Lysozyme†

Michael Blaber, Joel D. Lindstrom, Nadine Gassner, Jian Xu, Dirk W. Heinz, and Brian W. Matthews*

Institute of Molecular Biology, Howard Hughes Medical Institute, and Department of Physics, University of Oregon, Eugene, Oregon 97403

Received May 14, 1993; Revised Manuscript Received July 19, 1993®

ABSTRACT: In order to determine the thermodynamic cost of introducing a polar group within the core of a protein, a series of nine Ala → Ser and 3 Val → Thr substitutions was constructed in T4 lysozyme. The sites were all within α-helices but ranged from fully solvent-exposed to totally buried. The range of destabilization incurred by the Ala → Ser substitutions was found to be very similar to that for the Val → Thr replacements. For the solvent-exposed and partly exposed sites the destabilization was modest (≲0.5 kcal/mol). For the completely buried sites the destabilization was larger, but variable (~1–3 kcal/mol). Crystal structure determinations showed that the Ala → Ser mutant structures were, in general, very similar to their wild-type counterparts, even though the replacements introduce a hydroxyl group. This is in part because the introduced serines are all within α-helices and at congested sites can avoid steric clashes with surrounding atoms by making a hydrogen bond to a backbone carbonyl oxygen in the preceding turn of the helix. The three substituted threonine side chains essentially superimpose on their valine counterparts but display somewhat larger conformational adjustments. The results illustrate how a protein structure will adapt in different ways to avoid the presence of an unsatisfied hydrogen bond donor or acceptor. In the most extreme case, Val 149 → Thr, which is also the most destabilizing variant ($\Delta\Delta G$ = 2.8 kcal/mol), a water molecule is incorporated in the mutant structure in order to provide a hydrogen-bonding partner. The results are consistent with the view that many hydrogen bonds within proteins contribute only marginally to stability but that noncharged polar groups that lack a hydrogen-bonding partner are very destabilizing ($\Delta\Delta G \gtrsim 3$ kcal/mol). Supportive of other studies, the α-helix propensity of alanine is seen to be higher than that of serine ($\Delta\Delta G$ = 0.46 ± 0.04 kcal/mol), while threonine and valine are similar in α-helix propensity.

Downloaded via UNIV OF EDINBURGH on March 9, 2023 at 12:48:42 (UTC).
See https://pubs.acs.org/sharingguidelines for options on how to legitimately share published articles.

Following Pauling (1960) there has been little doubt as to the importance of hydrogen bonding in biological structures (Jeffrey & Saenger, 1991). At the same time, the strength of the hydrogen bond and the degree to which it contributes directly to the folding and stability of macromolecular structures have remained unclear (Klotz & Franzen, 1962; Roseman, 1988a,b; Sneddon et al., 1989). Some structural studies have suggested that hydrogen bonds can contribute directly and substantially to protein stability, while other such studies suggest that the directional requirements of hydrogen bonds (as opposed to hydrophobic interactions) help specify macromolecular structure rather than provide stability, *per se* (Fersht et al., 1985; Alber et al., 1987; Bartlett & Marlowe, 1987; Fersht, 1987). In the case of protein–ligand complexes, the energy contribution from hydrogen bonds requires an "accounting" of hydrogen-bonding possibilities in the free and liganded forms (Fersht, 1987; Bash et al., 1987). Similarly, in protein folding, consideration has to be given to both the folded and unfolded states.

Here we describe a series of nine Ala → Ser and 3 Val → Thr replacements in T4 lysozyme designed and constructed to investigate the introduction of a polar group in different environments in a typical globular protein. By choosing these replacements, the associated structural changes were expected to be minimal, especially in the case of Val → Thr. The hydroxyl group is small yet is adaptable in that it can act as a hydrogen bond donor or acceptor. Thermodynamic analysis of the mutant proteins provides the change in free energy associated with each substitution. Also for each of the 12 substitutions it was possible to determine the crystal structure of the mutant protein, making it possible to see how the protein adapted and to rationalize changes in stability in structural terms.

Related studies, without the benefit of detailed structural analysis, have been described by Marti et al. (1991) and Green et al. (1992).

MATERIALS AND METHODS

Pseudo-wild-type lysozyme, in which Cys residues at positions 54 and 97 have been replaced by Thr and Ala, respectively, was used as the reference protein and is referred to hereafter as WT* (Matsumura & Matthews, 1989).

Site Selection. In order to keep the analysis as simple as possible, substitutions were restricted to Ala → Ser and Val → Thr, using alanine or valine present in WT*. This allows the use of the WT* protein as the reference in every case. Both types of substitution allow the introduction of a hydroxyl group without the risk of large-scale perturbation of the structure.

The sites were also chosen to be within α-helical secondary structure. This was intended to keep all the sites comparable, at least so far as location within secondary structure was concerned. At the same time a variety of sites was chosen.

† This work was supported in part by grants from the National Institutes of Health (GM21967).

* To whom correspondence should be addressed.

® Abstract published in *Advance ACS Abstracts,* October 1, 1993.

0006-2960/93/0432-11363$04.00/0 © 1993 American Chemical Society

Table I: Mutant Location within the Local α-Helical Secondary Structure[a]

mutant	location in helix	residues within helix
Ala 41 → Ser	Ncap+3, Ccap-10	39–50
Ala 42 → Ser	Ncap+4, Ccap-9	39–50
Ala 44 → Ser[a]	Ncap+6, Ccap-7	39–50
Ala 49 → Ser	Ncap+11, Ccap-2	39–50
Ala 73 → Ser	Ncap+14, Ccap-7	60–79
Ala 82 → Ser	Ncap+1, Ccap-9	82–90
Ala 93 → Ser	Ncap+1, Ccap-14	93–106
Ala 98 → Ser	Ncap+6, Ccap-9	93–106
Ala 130 → Ser	Ncap+4, Ccap-5	126–134
Ala 131 → Ser[b]	Ncap+5, Ccap-4	126–134
Ala 134 → Ser	Ncap+9, Ccap-1	126–134
Val 44 → Thr[b]	Ncap+6, Ccap-7	39–50
Val 75 → Thr	Ncap+16, Ccap-5	60–79
Val 87 → Thr	Ncap+5, Ccap-4	82–90
Val 131 → Thr	Ncap+5, Ccap-4	126–134
Val 149 → Thr	Ncap+7, Ccap-7	143–155

[a] The N-cap and C-cap positions are defined as the first and last residues, respectively, in a region of α-helical secondary structure whose α-carbon atoms lie within the cylinder of the helix (Richardson & Richardson, 1988). The definition used for a residue to be "within a helix" is that it have (ϕ,ψ) values that correspond at least approximately to an α-helix and also participate in at least one helical hydrogen bond (Remington et al., 1978). [b] In WT* residue 44 is serine and residue 131 is valine. Therefore the three substitutions Ala 44 → Ser, Val 44 → Thr, and Ala 131 → Ser do not meet the standard requirement that the reference (parent) protein be WT*.

These included sites within the amino-terminal, central, and carboxyl-terminal regions of α-helices and solvent-exposed as well as solvent-inaccessible sites. A total of ten alanine residues and three valine residues met the above criteria (Table I). Additional Val → Thr and Ala → Ser mutations at sites 44 and 131 have been reported previously (Dao-pin et al., 1990; Blaber et al., 1993) and are included here for purposes of comparison.

Construction of Mutants and Purification of Proteins. Mutants were constructed using oligonucleotide-directed mutagenesis as described by Kunkel et al. (1987). The expression and purification of the mutant proteins was performed using previously described materials and methods (Alber & Matthews, 1987; Muchmore et al., 1989; Poteete et al., 1991).

Thermodynamic Analysis. Thermal stabilities were determined by monitoring the circular dichroism (CD) at 223 nm as a function of temperature, as described by Zhang et al. (1991). The thermodynamic parameters T_m, the melting temperature, and ΔH, the change in the enthalpy of unfolding at the melting temperature, were determined by averaging at least three measurements via the nonlinear fitting program NONLIN kindly provided by Dr. Michael Johnson (Johnson & Frasier, 1985). All measurements were in 25 mM KCl and 20 mM KPO_4, pH 3.0, in which the melting temperature of WT* was determined to be 51.55 ± 0.15 °C. The difference in melting temperature (ΔT_m) for each protein was calculated relative to WT*. The change in the free energy of unfolding, $\Delta\Delta G$, was calculated using the $\Delta T_m{}^*\Delta S$ approximation (Becktel & Schellman, 1987) as well as by using a model with temperature invariant ΔC_p = 2.5 kcal/(deg·mol) (Zhang et al., 1991). To facilitate comparison mutants reported previously were reevaluated under the conditions described.

Structure Determination. Crystals of each mutant were grown using conditions developed for the WT* protein (~2.0 M phosphate, pH 6.9; Weaver & Matthews, 1987). Isomorphous crystals (space group $P3_221$) were obtained in each case. High-resolution data sets for each mutant were collected using either oscillation photography (Rossmann, 1979; Schmid et al., 1981) or a multiwire area detector (Hamlin, 1985). All structures were refined using the TNT least-squares refinement package (Tronrud et al., 1987; Tronrud, 1992).

Table II: Thermal Stabilities of Mutant Lysozymes[a]

mutant	T_m (°C)	ΔT_m (°C)	ΔH (kcal/mol)	ΔS (entropy units)	$\Delta T_m\Delta S$ (kcal/mol)	$\Delta\Delta G$ (kcal/mol)
Ala 41 → Ser	49.78	−1.77	106	329	−0.6	−0.6
Ala 42 → Ser	44.06	−7.49	89	281	−2.1	−2.3
Ala 49 → Ser	50.02	−1.53	110	340	−0.5	−0.5
Ala 73 → Ser	50.28	−1.27	111	344	−0.4	−0.4
Ala 82 → Ser	50.56	−0.99	112	347	−0.3	−0.3
Ala 93 → Ser	51.03	−0.52	112	346	−0.2	−0.2
Ala 98 → Ser	44.08	−7.47	97	306	−2.3	−2.5
Ala 130 → Ser	48.66	−2.89	107	332	−1.0	−1.0
Ala 134 → Ser	51.11	−0.44	111	342	−0.1	−0.1
Val 75 → Thr	47.85	−3.70	113	351	−1.3	−1.3
Val 87 → Thr	47.00	−4.55	105	329	−1.5	−1.6
Val 149 → Thr	41.47	−10.08	77	244	−2.5	−2.8
WT* (control)	51.55		113	349		

[a] T_m is the melting temperature of the protein (estimated uncertainty 0.15 °C) and ΔT_m the difference between the T_m of the mutant and that of WT*. ΔH is the enthalpy of unfolding at the T_m of the mutant (estimated uncertainty 5 kcal/mol). ΔS is the entropy of unfolding at the T_m of the mutant. $\Delta\Delta G$ was estimated using the $\Delta T_m{}^*\Delta S$ approximation as well as by a constant ΔC_p model (see text).

RESULTS

Thermodynamic Data. All of the mutants exhibited reversible unfolding with 90% or better restoration of CD signal upon cooling. Table II summarizes the thermodynamic data. Values for $\Delta\Delta G$ estimated from $\Delta T_m{}^*\Delta S$ agree well with values calculated using a constant ΔC_p model, especially when ΔT_m is small. The values for ΔH decrease with melting temperature with the lowest ΔH value observed for Val 149 → Thr, the least stable mutant. As will be described below, Val 149 → Thr is structurally unique in that a solvent group is sequestered in the core of the protein.

Structures of Mutant Lysozymes. Crystallographic data are summarized in Table III. The location of the introduced hydroxyl group in the Ala → Ser mutants was unambiguous in the initial $F_{mutant} - F_{WT*}$ density maps for all mutants except for the Ala 82 → Ser and Ala 93 → Ser (see below). In the case of the Val → Thr mutants, the $F_{mutant} - F_{WT*}$ density maps (F_{mutant} and F_{WT*} being observed structure amplitudes; phases from WT*) were generally devoid of features indicating that the new Thr side chain in every case essentially superimposed on the isostructural valine.

All the refined mutant structures are, in general, very similar to that of WT*. The root-mean-square (rms) deviation for all main-chain atoms ranged from 0.08 to 0.17 Å (Table IV). This is within the estimated positional error (~0.15 Å). To evaluate possible changes in structure close to the site of mutation, the deviation was calculated for main-chain atoms within an 8-Å radius of the hydroxyl oxygen of the substituted side chain. These deviations closely parallel the values for the structure as a whole (Table IV), showing that the structure in the vicinity of each substitution is also similar to WT*.

Ala 41 → Ser. This site is relatively solvent-exposed and is located at the (Ncap+3) location of α-helix 39–50 (Table I). As a consequence the (*i*–4) main-chain carbonyl is not in a position to serve as a hydrogen-bonding partner. The γ-hydroxyl of the introduced serine side chain adopts a χ_1 angle of 158° (Table IV), which is reasonably close to one of the preferred low energy values (±180°). The hydroxyl group hydrogen bonds with the side-chain carbonyl of Asn 116 in a symmetry-related molecule (Figure 1, Table V). In solution

Table III: X-ray Data Collection and Refinement Statistics[a]

mutant	cell dimensions *a,b* (Å)	cell dimensions *c* (Å)	data collection method	independent reflections	R_{merge} (%)	resolution (Å)	data completeness (%)	*R* (%)	bond length deviation (Å)	bond angle deviation (deg)
Ala 41 → Ser	61.3	97.2	osc. film	14 462	9.8	1.80	70	16.2	0.018	2.2
Ala 42 → Ser	61.0	97.0	area det.	18 840	3.4	1.75	82	16.4	0.014	2.0
Ala 49 → Ser	61.1	97.0	osc. film	15 924	5.7	1.70	67	15.8	0.017	2.1
Ala 73 → Ser	60.9	96.8	area det.	17 941	3.0	1.80	87	14.9	0.017	2.0
Ala 82 → Ser	60.8	97.0	area det.	16 781	2.8	1.80	84	15.0	0.016	2.0
Ala 93 → Ser	61.1	97.0	osc. film	14 791	7.0	1.85	71	16.4	0.016	2.2
Ala 98 → Ser	60.9	96.9	area det.	15 492	2.4	1.85	82	14.4	0.015	2.0
Ala 130 → Ser	60.8	97.0	area det.	18 037	2.9	1.80	87	14.6	0.016	2.0
Ala 134 → Ser	61.3	97.3	osc. film	17 057	6.4	1.65	65	16.2	0.017	2.0
Val 75 → Thr	60.7	97.6	area det.	15 800	2.8	1.85	84	14.3	0.016	2.0
Val 87 → Thr	61.3	97.4	osc. film	15 649	6.7	1.70	65	16.1	0.017	2.0
Val 149 → Thr	61.0	96.5	area det.	17 805	3.3	1.80	87	15.5	0.015	1.9
WT*	60.8	96.8								

[a] The WT* structure has previously been described (Matsumura & Matthews, 1989). All mutants crystallized in the WT*($P3_221$) space group with $\alpha = \beta = 90°$ and $\gamma = 120°$.

Table IV: Comparison of Mutant and WT* Structures[a]

mutant	difference between mutant structures and WT* (Å): residues 1–160 (whole molecule)	difference between mutant structures and WT* (Å): atoms within 8-Å radius of mutation site	conformation at substitution site (deg): wild-type main chain ϕ	wild-type main chain ψ	wild-type side chain χ_1	mutant main chain ϕ	mutant main chain ψ	mutant side chain χ_1
Ala 41 → Ser	0.16	0.14	−65	−31		−64	−36	158
Ala 42 → Ser	0.09	0.09	−66	−44		−63	−46	101
(Ser 44 → Ala)[b]	0.11	0.16						
Ala 49 → Ser	0.08	0.07	−66	−37		−67	−39	−66
Ala 73 → Ser	0.08	0.07	−61	−43		−64	−42	−63
Ala 82 → Ser	0.10	0.10	−65	−28		−60	−26	120
Ala 93 → Ser	0.09	0.06	−59	−39		−62	−38	49/−99
Ala 98 → Ser	0.12	0.10	−61	−42		−64	−41	−103
Ala 130 → Ser	0.10	0.08	−62	−43		−62	−39	−68
Ala 134 → Ser	0.13	0.06	−71	−20		−72	−19	75
Val 75 → Thr	0.17	0.15	−53	−50	−61	−62	−48	−48
Val 87 → Thr	0.16	0.16	−64	−52	−53	−67	−49	−55
Val 131 → Thr[d]	0.12	0.25						
Val 149 → Thr	0.11	0.10	−66	−45	−66	−68	−44	−61

[a] The first two entries give the root-mean-square discrepancy between each mutant and WT*, for main-chain atoms of the entire molecule (residues 1–160), and for the region within an 8-Å radius of the site of substitution. [b] From Blaber et al. (1993). [c] The side chain of Ser 93 displayed two alternate conformations (see text). The structure was refined in the predominant conformation. [d] From Dao-pin et al. (1990).

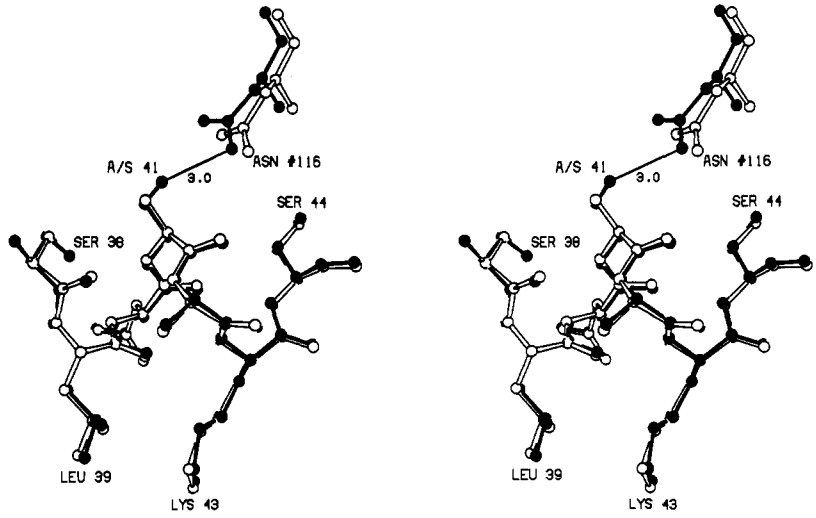

FIGURE 1: Structure of the Ala 41 → Ser mutant (solid bonds) in the region of the mutation overlaid on the WT*(Ala) structure (open bonds). Asn #116 is from a neighboring molecule in the crystal lattice.

this symmetry-related hydrogen-bonding partner would not be present and would presumably be replaced by solvent.

Ala 42 → Ser. The side-chain γ-hydroxyl at this site is completely buried. This site is at the (Ncap+4) position so that the main-chain carbonyl at the (*i*–4) position is a potential hydrogen-bonding partner (Janin et al., 1978; Gray & Matthews, 1984). However, the Ser 42 side chain is observed to hydrogen bond with the main-chain carbonyl at the (*i*–3) position (Figure 2, Table V). In order to do so, the side chain adopts a χ_1 angle of 101° (Table IV) which results in a strained

Table V: Hydrogen-Bonding Geometry for the γ-Hydroxyl Group of the Mutant Ser and Thr Residues[a]

mutant	hydrogen bond partner	distance (Å)	atom group	angle (deg)
Ala 41 → Ser, O^{γ}	$O^{\delta 1}$ Asn 116 (sym. related)	3.0	C^{β} 41 O^{γ} 41...$O^{\delta 1}$ 116	114
			C^{γ} 116 $O^{\delta 1}$ 116...O^{γ} 41	114
Ala 42 → Ser, O^{γ}	O 39	2.9	C^{β} 42 O^{γ} 42...O 39	102
			C 39 O 39...O^{γ} 42	117
Ala 49 → Ser, O^{γ}	O 45	3.1	C^{β} 49 O^{γ} 49...O 45	92
			C 45 O 45...O^{γ} 49	137
	OH 200 (sol)	2.9	C^{β} 49 O^{γ} 49...OH 200	139
Ala 73 → Ser, O^{γ}	O 69	3.0	C^{β} 73 O^{γ} 73...O 69	101
			C 69 O 69...O^{γ} 73	148
	OH 201 (sol)	3.0	C^{β} 73 O^{γ} 73...OH 201	142
Ala 82 → Ser, O^{γ}	OH 336 (sol)	2.4	C^{β} 82 O^{γ} 82...OH 336	126
Ala 93 → Ser, O^{γ}	OH 177 (sol), $\chi_1 = 49°$	3.0	C^{β} 93 O^{γ} 93...OH 177	117
	OH 185 (sol), $\chi_1 = -99°$	2.4	C^{β} 93 O^{γ} 93...OH 185	137
Ala 98 → Ser, O^{γ}	O 149	3.1	C^{β} 98 O^{γ} 98...O 149	128
			C 149 O 149...O^{γ} 98	125
Ala 130 → Ser, O^{γ}	O 126	2.9	C^{β} 130 O^{γ} 130...O 126	96
			C 126 O 126...O^{γ} 130	147
Ala 134 → Ser, O^{γ}	O 131	2.8	C^{β} 134 O^{γ} 134...O 131	118
			C 131 O 131...O^{γ} 134	130
	OH 251 (sol)	3.0	C^{β} 134 O^{γ} 134...OH 251	151
Val 75 → Thr, $O^{\gamma 1}$	O 71	2.9	C^{β} 75 $O^{\gamma 1}$ 75...O 71	104
			C 71 O 71...$O^{\gamma 1}$ 75	143
Val 87 → Thr, $O^{\gamma 1}$	$O^{\epsilon 1}$ Gln 122	2.8	C^{β} 87 $O^{\gamma 1}$ 87...$O^{\epsilon 1}$ 122	142
			C^{δ} 122 $O^{\epsilon 1}$ 122...$O^{\gamma 1}$ 87	108
Val 149 → Thr, $O^{\gamma 1}$	OH 323 (sol)	2.8	C^{β} 149 $O^{\gamma 1}$ 149...OH 323	158

[a] The hydrogen-bonding interactions for both orientations of the Ser 93 mutant are shown (see text).

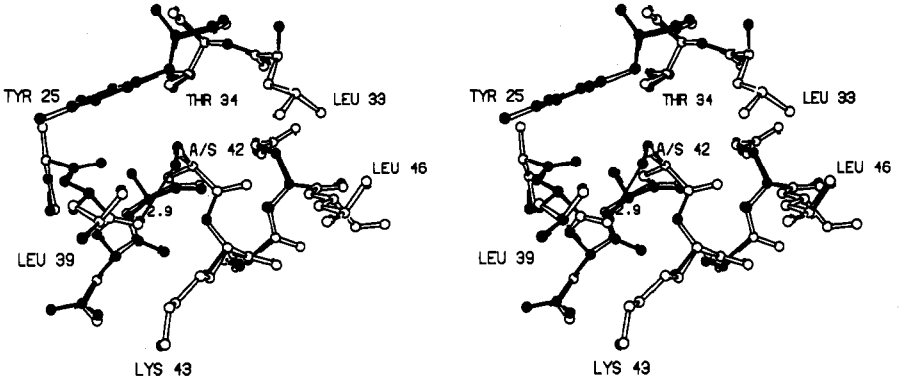

FIGURE 2: Structure of the Ala 42 → Ser mutant (solid) in the region of site 42 overlaid on the WT*(Ala) structure (open bonds).

conformation due to the eclipsing of the main-chain carbon by the side-chain γ-hydroxyl. Modeling studies of this mutant indicate that a low-energy rotamer conformation of $\chi_1 = -60°$, which would in principle allow an (*i*–4) hydrogen bond, would incur prohibitively close contacts of 2.5 Å with the $C^{\gamma 2}$ atom of Thr 34 and 2.7 Å with the $C^{\delta 1}$ atom of Tyr 25. An alternative low-energy χ_1 angle of ±180° would result in less severe neighbor contact distances of 3.0 Å with the C^{β} atom of Tyr 25 and 3.26 Å with the $C^{\delta 2}$ atom of Leu 33. In this orientation, however, no hydrogen-bonding partners are apparent. Thus, the core environment at this site does not appear to be able to accommodate the O^{γ} of the mutant Ser side chain in either of the preferred rotamer orientations, either for steric or hydrogen-bonding reasons. The observed (*i*–3) hydrogen-bonding arrangement, although resulting in a strained χ_1 angle, provides a hydrogen-bonding partner and obviates rearrangement of the local structure. The strained structure is consistent with the fact that this is one of the most destabilizing Ala → Ser replacements ($\Delta\Delta G$ = –2.3 kcal/mol).

Ala 49 → Ser. This site is located toward the carboxyl terminus of the local helix (Table I). The side chain adopts a nearly ideal χ_1 angle of –66° (Table IV) which orients the side-chain γ-hydroxyl group toward the main-chain (*i*–4) carbonyl. The side-chain γ-hydroxyl is within hydrogen-bonding distances of both the (*i*–4) main-chain carbonyl (3.1 Å) and a solvent group (Sol 200, 2.9 Å; Figure 3, Table V). The side-chain γ-hydroxyl is partly solvent exposed and forms a hydrogen bond to Sol 200.

Ala 73 → Ser. Ala 73 is located in the central part of the longest helix of T4 lysozyme (Table I). The side chain of Ser 73 adopts a near ideal χ_1 angle (–63°, Table IV) which orients the γ-hydroxyl toward and within hydrogen-bonding distance of the (*i*–4) main-chain carbonyl as well as a solvent molecule (Sol 201; Figure 4, Table V). A very similar hydrogen-bonding arrangement is also seen for the site Ala 49 → Ser mutant.

Ala 82 → Ser. This site is located at the (Ncap+1) position in the helix 82–90 (Table I), and, like site 41, there is no (*i*–4) main-chain carbonyl available as a hydrogen-bonding partner and the Ser γ-hydroxyl is hydrogen-bonded to a solvent molecule (Figure 5, Table V). This is one of the more accessible sites evaluated. In the refined model the γ-oxygen of Ser 82 has a crystallographic *B* factor of 54 $Å^2$, suggesting that the side chain is quite mobile and possibly occupies more than one rotamer angle. Model building suggests that χ_1 values of either –60° or ±180° would not lead to any apparent steric conflicts and would leave the side-chain γ-hydroxyl relatively accessible to solvent. The refined χ_1 angle for Ser 82 is 120° (Table IV) which corresponds to an eclipsed conformation. As noted, however, the side chain is mobile, and the value of 120° is therefore not well defined.

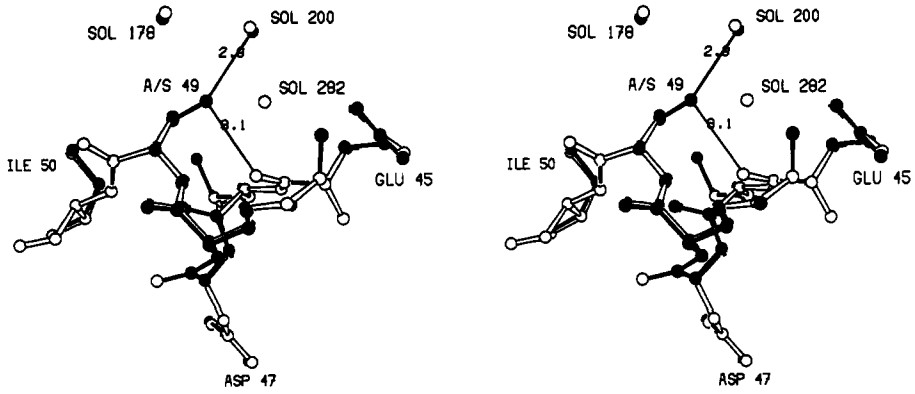

FIGURE 3: Structure of the Ala 49 → Ser mutant (solid) in the region of site 49 overlaid on the WT*(Ala) structure (open bonds).

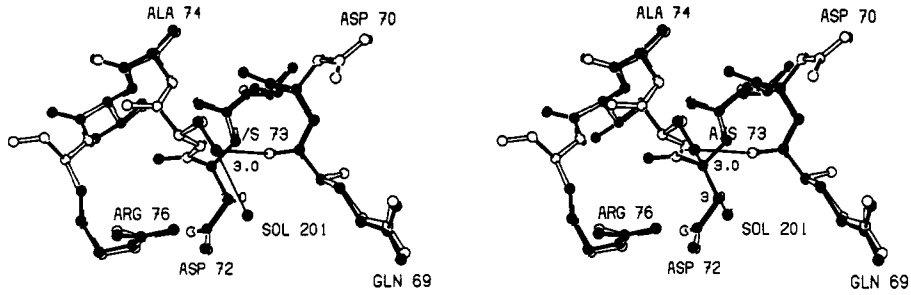

FIGURE 4: Structure of the Ala 73 → Ser mutant (solid) in the region of residue 73 superimposed on the WT*(Ala) structure (open).

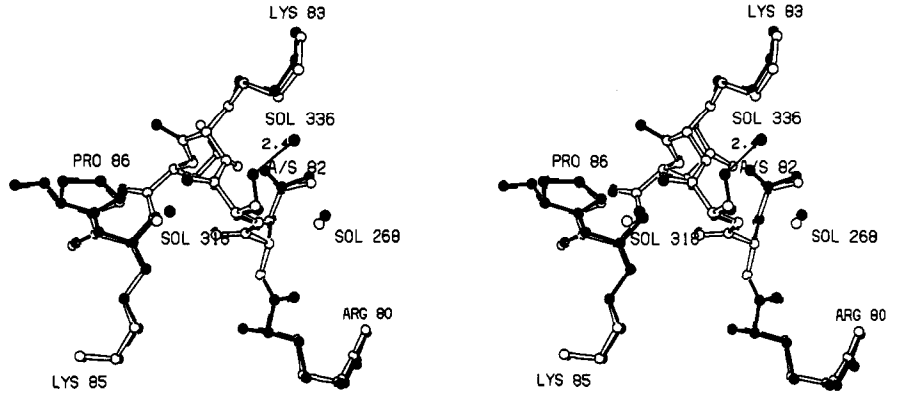

FIGURE 5: Structure of the Ala 82 → Ser mutant (solid) in the region of the substitution overlaid on the WT*(Ala) structure (open).

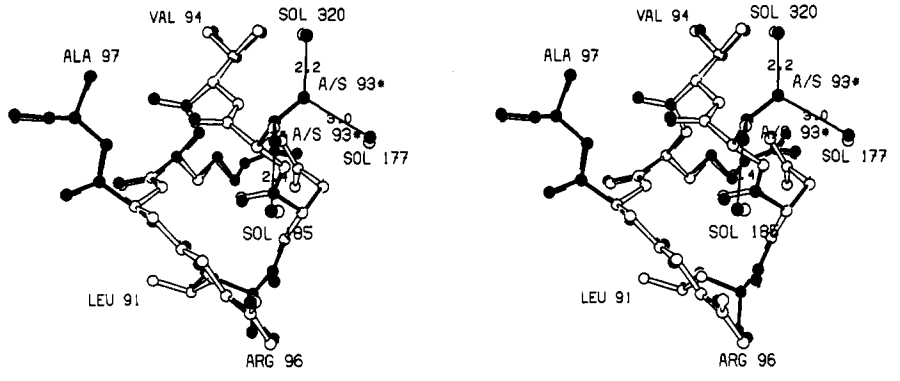

FIGURE 6: Structure of the Ala 93 → Ser mutant (solid) in the region of site 93 overlaid with the WT*(Ala) structure (open). The γ-oxygen of Ser 93 appears to occupy two alternative positions labeled A/S93 and A/S93*.

Ala 93 → Ser. Residue 93 is located close to the amino terminus (Ncap+1) of the local helix. In this mutant two regions of electron density attributable to the O^{γ} group were apparent and were interpreted as two possible orientations for the O^{γ}. Crystallographic refinement supports this conclusion (Table IV, Figure 6). The two alternative conformations of the γ-hydroxyl group correspond to χ_1 angles of 49° and −99° (Table IV). In both orientations the γ-hydroxyl hydrogen bonds to solvent (Figure 6, Table V). At a χ_1 angle of −60° the side-chain γ-hydroxyl group would have a close contact (2.8 Å) with the C^{γ} atom at position 69 in a symmetry-related molecule. At χ_1 equal to ±180° the side-chain hydroxyl would likewise have a close contact (3.0 Å) with the C^{β} atom of Asn 68 in a symmetry-related molecule. It is not clear to what

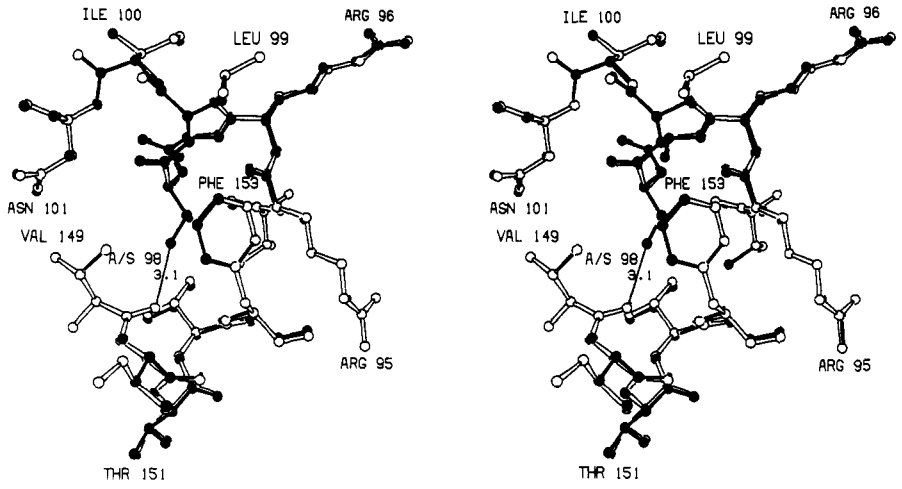

FIGURE 7: Structure of the Ala 98 → Ser site 98 Ser mutant (solid) in the region of site 98 overlaid on the WT*(Ala) structure (open).

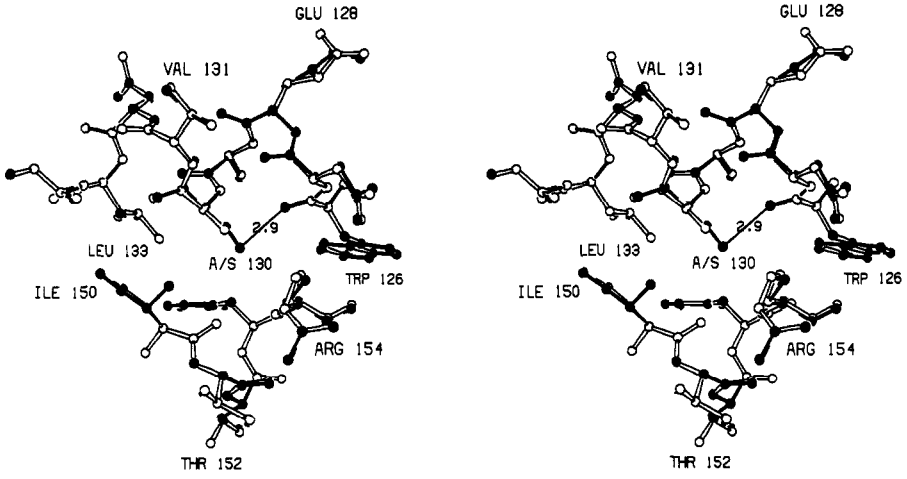

FIGURE 8: Structure of the Ala 130 → Ser site 130 Ser mutant (solid) in the region of site 130 overlaid the WT*(Ala) structure (open).

extent the presence of these symmetry-related atoms influence the observed conformations at this site.

Ala 98 → Ser. This site is located within the central region of the helix 92–106 (Table I) and is completely solvent-inaccessible. Although the main-chain (*i*–4) carbonyl is included in the local helical structure, it does not participate in a hydrogen-bonding interaction with the side-chain γ-hydroxyl. Instead, the serine hydroxyl interacts with the main-chain carbonyl of Val 149 on the buried face of a neighboring α-helix (residues 142–156; Figure 7, Table V). The location of the serine hydroxyl relative to the neighboring helix is similar to the site that solvent atoms commonly occupy on the solvent-accessible face of an α-helix, i.e., positioned "above" the main-chain intrahelical hydrogen bond and hydrogen bonding with the main-chain carbonyl (Sundaralingam & Sekharudu, 1989). Thus, within the core of the protein is a hydrogen-bonding interaction reminiscent of those seen at the solvent-exposed surfaces of helices. The serine side chain adopts a somewhat strained χ_1 angle of −103°, and modeling suggests that the preferred χ_1 angles of −60° or ±180° would result in close contacts with neighbor groups. At a χ_1 angle of −60°, which could allow the (*i*–4) main-chain carbonyl to participate as a hydrogen-bonding partner, the side-chain hydroxyl has a close contact (2.9 Å) with the $C^{\gamma 2}$ atom of Ile 150. At a χ_1 angle of ±180° the side-chain hydroxyl has close contacts with the $C^{\gamma 1}$ atom of Val 149 (2.9 Å) and the $C^{\epsilon 2}$ atom of Phe 153 (2.7 Å). The strained geometry is again consistent with the observed destabilization ($\Delta\Delta G$ = −2.5 kcal/mol).

Ala 130 → Ser. Site 130 is located in the center of α-helix 126–134 (Table I) and the side-chain hydroxyl is completely solvent-inaccessible. The Ser side chain adopts a χ_1 angle of −68° (Table IV) which is close to a low-energy orientation (−60°) and the side-chain γ-hydroxyl and hydrogen-bonded to the (*i*–4) main-chain carbonyl (Figure 8, Table V). The serine side chain is accommodated with little, if any, indication of strain or distortion (Table IV, Figure 8).

Ala 134→Ser. This site is located at the carboxyl terminal region of α-helix 125–135 (Table I). Although the (*i*–4) main-chain carbonyl is included within the helix, the serine side chain adopts a χ_1 angle of 75° (Table IV) and participates in a hydrogen-bonding interaction with the main-chain carbonyl at the (*i*–3) position, in addition to a local solvent molecule (Figure 9, Table V). Although the (*i*–3) type of hydrogen-bonding interaction is similar to that in the Ser 42 mutant, the structural basis is fundamentally different. At site 134 the α-helical secondary structure ends (site 134 being the last residue with ψ,φ angles characteristic of an α-helix) and begins a turn into a short helical region (residues 137–141). As a consequence, in the WT* structure the main-chain carbonyl at Val 131 hydrogen bonds to solvent rather than to a main-chain amide at position 135. Consequently, the region around the main-chain carbonyl of Val 131 is solvent-exposed and relatively unobstructed in the WT* structure. The side-chain hydroxyl group of the mutant Ser 134 is positioned within this area and by adopting the χ_1 angle of 75° hydrogen bonds with the carbonyl oxygen of Val 131

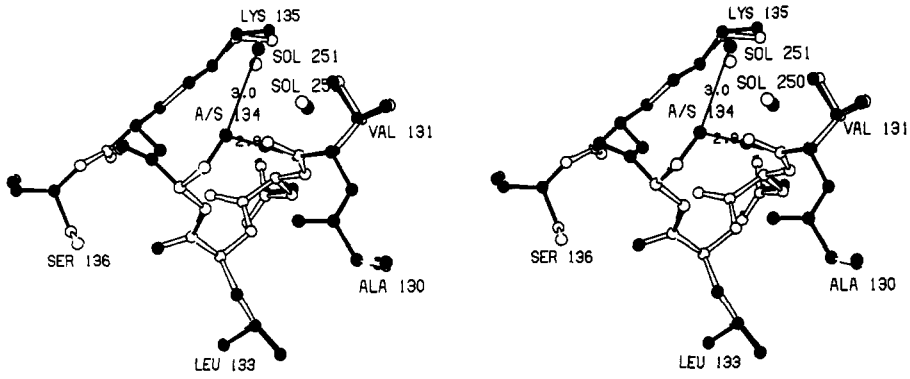

FIGURE 9: Structure of the Ala 134 → Ser mutant (solid) in the region of the substitution superimposed on the WT*(Ala) structure (open).

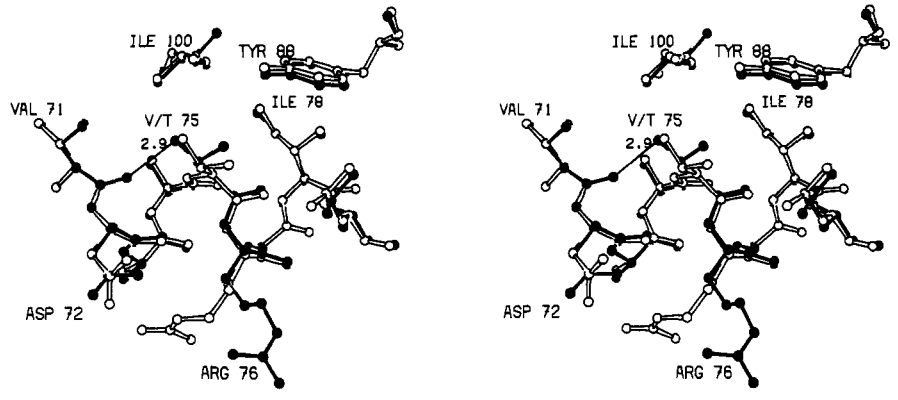

FIGURE 10: Structure of the Val 75 → Thr mutant (solid) in the region of site 75 overlaid on the WT*(Val) structure (open).

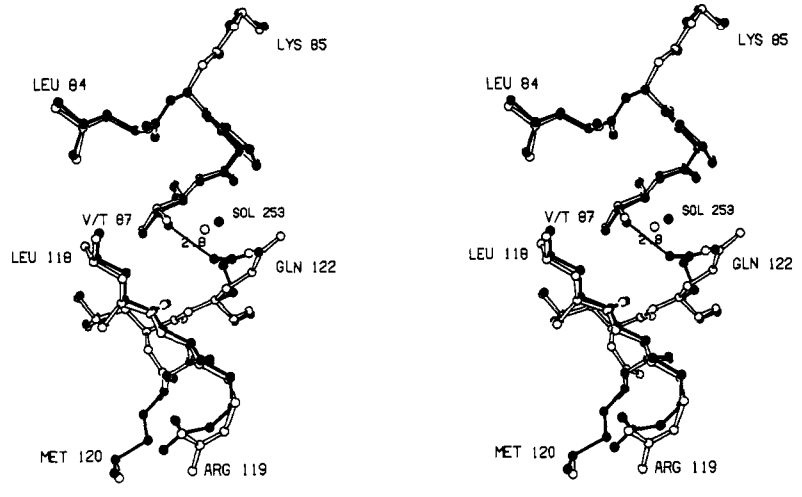

FIGURE 11: Structure of the Val 87 → Thr mutant (solid) in the region of site 87 overlaid on the WT*(Val) structure (open).

(Figure 9). This χ_1 angle therefore is not as strained as it would be if the helix extended through site 135, and the hydrogen-bonding requirements of both the side-chain hydroxyl and site 131 main-chain carbonyl are satisfied.

Val 75 → Thr. This site is located within the "long helix" (residues 60–79) of T4 lysozyme (Table I). The mutant Thr side chain adopts a conformation very similar to that of the WT* valine (Figure 10). The most noticeable difference is a rotation about χ_1 of approximately +13°, which brings the $O^{\gamma 1}$ hydroxyl into closer proximity to the (*i*–4) main-chain carbonyl. The side-chain hydroxyl is hydrogen bonded only to this carbonyl and not to any solvent groups (Table V). The site is almost entirely solvent-inaccessible.

Val 87 → Thr. Site 87 is located toward the carboxyl terminus of helix 82–90 (Table I) and is solvent-inaccessible. The mutant threonine side-chain superimposes on that of the WT* valine (Figure 11), with the χ_1 angles in the mutant and WT* structures being essentially identical. Although the helical secondary structure extends through the (*i*–4) position the mutant threonine side-chain hydroxyl does not participate in a hydrogen bond with the (*i*–4) main-chain carbonyl. This is due to the presence of the neighboring residue Pro 86. This residue introduces a slight distortion in the helix, as a result of which the main-chain carbonyl at Lys 83 is greater than 3.6 Å from the Val/Ala 87 amide nitrogen in both the mutant and WT* structures. Thus, although the helical region is defined by α-carbons from residues 82–90, it is somewhat distorted for the first few residues. In response to the introduction of a threonine at site 87, the side chain of Gln 122 moves to participate as a hydrogen-bonding partner. In the WT* structure Gln 122 adopts a χ_1 angle of −171°. In the threonine mutant the χ_1 angle is -75 Å which positions

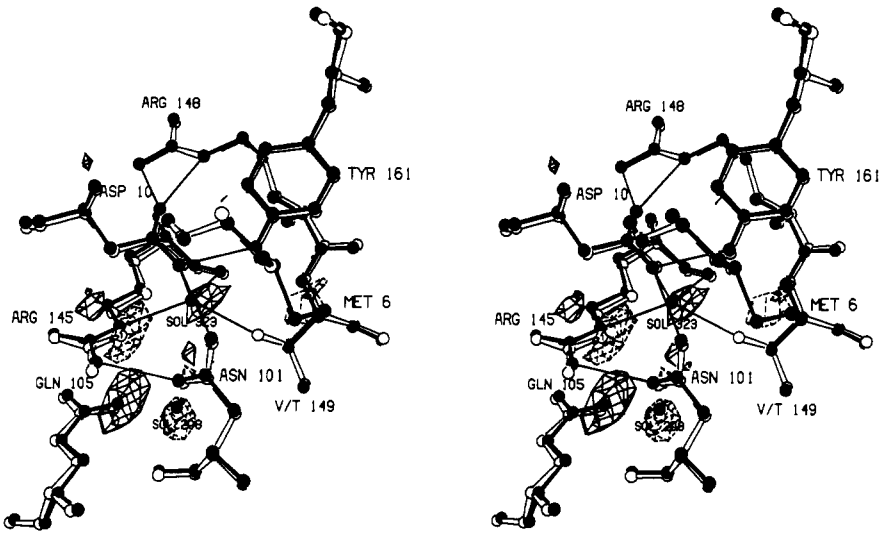

FIGURE 12: Structure of the Val 149 → Thr mutant (solid) in the region of site 149 superimposed on the WT*(Val) structure (open). The figure includes the electron density map showing the solvent molecule (#323) bound in the mutant structure. Coefficients ($F_{mut} - F_{WT}$) where F_{mut} and F_{WT} are the observed structure amplitudes for the mutant and wild-type structures. Phases are from the refined structure of wild-type lysozyme. The map is contoured at 4σ (solid) and -4σ (broken) where σ is the root mean square density throughout the unit cell.

the $O^{\epsilon 1}$ atom 2.8 Å from the $O^{\gamma 1}$ group of Thr 87 (Figure 11, Table V). Gln 122 is located in the helix 115–123 so that the two alternative χ_1 angles are close to low-energy rotamer positions. The alteration in χ_1 angles for the Gln 122 side chain results in a decrease of approximately 13 Å^2 in accessible area. Thus, in response to the substitution of valine by threonine, a neighboring side chain becomes partially buried to provide a hydrogen-bonding partner. This movement is accomplished with virtually no distortion of the local structure (Table IV, Figure 11).

Val 149 → Thr. Site 149 is located in the center of the helix 143–155 (Table I) and is completely buried. The mutant threonine side chain virtually superimposes on the WT* valyl residue (Figure 12) and does not undergo any significant change in χ_1 to bring the $O^{\gamma 1}$ group closer to the (i–4) main-chain carbonyl. The distance between this atom and the γ-oxygen is 3.4 Å, suggesting that their interaction is weak at best. At the same time, however, there is a short contact distance of 2.7 Å between the $O^{\gamma 1}$ group and main-chain amide of the same residue (i.e., Thr 149). This is the shortest such approach observed for all mutants. If the Thr 149 side chain is rotated from $\chi_1 = -61°$ to $\chi_1 = -45°$, the contact distance decreases to approximately 2.5 Å while the $O^{\gamma 1}$ to (i–4) carbonyl distance approaches 3.0 Å. Therefore, the structure of this helix appears to be such that a close contact exists between the main-chain amide at position 149 and side-chain $O^{\gamma 1}$ group, and this precludes a strong (i–4) hydrogen bond.

The most striking feature of this mutant is the inclusion of a buried solvent molecule (SOL 323) which serves as a hydrogen-bonding partner for the substituted threonine (Figure 12, Table V). The protein accommodates this solvent molecule with modest distortions of the local structure, the largest being in the side-chain of Arg 145, which shifts approximately 0.25 Å (Figure 12). The solvent molecule is located "above" the intrachain hydrogen bond between the main-chain carbonyl at Arg 145 and the main-chain amide of Thr 149 and is within hydrogen-bonding distance (3.1 Å) of the Arg 145 carbonyl. The site occupied by the solvent group is therefore very similar to that observed for solvent groups interacting with solvent-accessible surfaces of α-helices (Sundaralingam & Sekharudu, 1989). In addition to the mutant $O^{\gamma 1}$ group and Arg 145 main-chain carbonyl, the solvent molecule has favorable hydrogen-bonding geometry with the N^{ϵ} atom of Arg 145 (Figure 12). Although the mutant $O^{\gamma 1}$ group has a close contact (2.6 Å) with the $O^{\delta 2}$ atom of Asp 10, the geometry is poor for a hydrogen bond and $O^{\delta 2}$ of Asp 10 interacts primarily with the O^{η} hydroxyl of Tyr 161 and the $N^{\delta 2}$ atom of Asn 101, the position of these atoms being virtually unchanged in the WT* and mutant structures. All of these groups are involved in other hydrogen-bonding interactions in the WT* structure which seem to be maintained in the mutant structure. The binding site of the solvent molecule in the mutant structure is relatively polar, which permits several hydrogen bonds, in addition to that introduced by the mutation (Figure 12).

DISCUSSION

Ala → Ser Substitutions. The $\Delta\Delta G$ values vs the solvent-accessible areas (Lee & Richards, 1970) of the introduced side-chain γ-hydroxyl for the Ala → Ser mutants are plotted in Figure 13a. Included in this plot are data derived from a previously described Ser → Ala mutant at site 44 (Heinz et al., 1992). This site is located centrally on the solvent-exposed face of helix 39–50 and was used for a study of helical propensity (Blaber et al., 1993). The immediate inference from Figure 13a is that the only substitutions that cause substantial changes in stability are those at buried sites. Mutants for which the side-chain γ-hydroxyl has an accessible area larger than approximately 15 Å^2 (i.e., about one-third or more exposed to solvent) exhibit modest changes in stability. For several of the mutants in this category, an additional manifestation of "solvent accessible" is provided by crystallographically localized solvent that participates in hydrogen-bonding interactions with the mutant side chain (Table V).

Those solvent-exposed sites that are free of other influence permit estimates to be obtained of the relative helix propensity of the substituted residues. There are three sites, 44, 49, and 73, that are located centrally within an α-helix (at least four residues from either terminus) and are relatively solvent-exposed. For these three sites $\Delta\Delta G$ for the serine substitutions relative to alanine is -0.46 ± 0.04 kcal/mol. This agrees remarkably well with $\Delta\Delta G$ values of -0.51 kcal/mol (Lyu et al., 1990) and -0.42 kcal/mol (O'Neil & Degrado, 1990) obtained using model peptide systems. Including the other sites that are also relatively solvent-exposed but are located

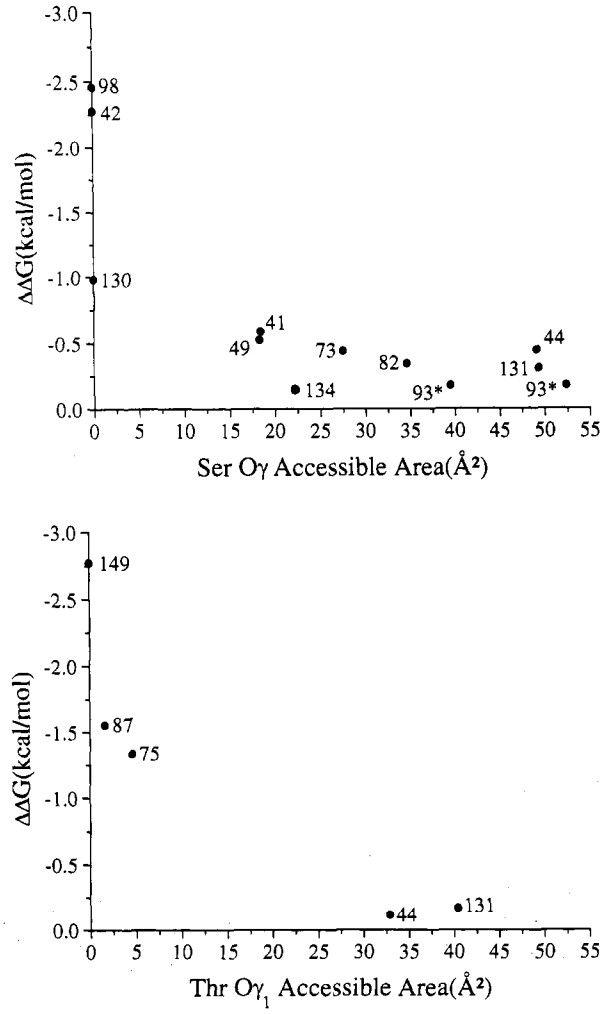

FIGURE 13: (a) Change in protein stability ($\Delta\Delta G$ from Table II) for Ala → Ser mutants plotted as a function of the solvent accessible surface area (Lee & Richards, 1970) of the O^{γ} atom. Ser 93 exhibits two possible conformations (see text), and the solvent accessibility for each of these orientations is indicated with an asterisk. $\Delta\Delta G$ for a Ser → Ala mutation at site 44 (Heinz et al., 1992) was redetermined under the conditions of this study and is included for comparison. The $\Delta\Delta G$ value for this mutant is reversed in sign to indicate the direction of substitution from Ala → Ser (see text). (b) Similar plot of the $\Delta\Delta G$ values vs the accessible areas of the $O^{\gamma 1}$ atom in Val → Thr substitutions. Included in this plot are substitutions at sites 44 and 131 of T4 lysozyme (Blaber et al., 1993; Dao-pin et al., 1990).

toward the ends of helices (sites 41, 82, 93, and 134), the individual changes in stability are somewhat less consistent with an average $\Delta\Delta G$ of -0.38 ± 0.16 kcal/mol.

Although several of the Ala → Ser substitutions result in the introduction of new (i.e., intrahelical) hydrogen bonds not present in wild-type, they do not increase protein stability. This clearly suggests that the introduction of new hydrogen bonds into a folded protein structure does not necessarily increase the stability of the folded relative to the unfolded form. It also helps explain why serine and threonine have relatively low α-helix propensity. They can participate in intrahelical hydrogen bonding but may do so because this is the lowest energy option available. The resultant conformation may be under strain and the hydrogen bonds of nonideal geometry. To the extent that the hydroxyl of the serine or threonine forms a hydrogen bond with a backbone carbonyl oxygen in the preceding turn of the α-helix, it may weaken the "α-helical" hydrogen bond in which the carbonyl oxygen is already participating. Under such circumstances an intrahelical hydrogen bond formed by a serine or threonine need not necessarily increase the stability of the helical structure relative to the unfolded protein.

The substitutions at buried sites, 42, 98, and 130 (Figure 13a), are all more destabilizing than the solvent-exposed ones. They also exhibit a much wider range of $\Delta\Delta G$ values, from approximately -1.0 kcal/mol for site 130 to -2.5 kcal/mol for both sites 42 and 98 (Table II). The most destabilizing substitutions (Ala 42 → Ser and Ala 98 → Ser) are seen to introduce strain into the folded protein.

The three buried Ala → Ser substitutions each reduce the volume of cavities that exist in the native protein by 11–16 Å^3. This corresponds to an expected stabilization of about 0.3–0.5 kcal/mol (Eriksson et al., 1992). At the same time the loss in hydrocarbon surface area associated with a buried Ala → Ser replacement corresponds to a destabilization of about 0.5 kcal/mol. The energetic consequences of cavity reduction and the hydrophobic effect in the case of the Ala → Ser replacements are, therefore, modest and roughly offsetting.

Val → Thr Substitutions. The plot of $\Delta\Delta G$ vs solvent accessibility for the Val → Thr substitutions (Figure 13b) is remarkably similar to that for the Ala → Ser replacements (Figure 13a). Included in Figure 13b are valine and threonine variants previously described for sites 44 and 131 (Dao-pin et al., 1990; Blaber et al., 1993). The set of Val → Thr mutants is more limited than the Ala → Ser series, but the general conclusions appear to be the same. The $\Delta\Delta G$ values for the mutants at sites considered to be "solvent accessible" are -0.11 kcal/mol for site 44 and -0.17 kcal/mol for site 131 (Table II, Figure 13b). These values are similar to the helical propensities of threonine relative to valine obtained from studies of small peptides [-0.11 kcal/mol, (Lyu et al., 1990); -0.03 kcal/mol, (O'Neil & DeGrado, 1990)].

At solvent-inaccessible sites the $\Delta\Delta G$ values are significantly greater in magnitude, ranging from approximately -1.3 kcal/mol at site 75 to -2.8 kcal/mol at site 149. Although the local helix extends through the (i–4) position in each of these cases, only the Thr 75 γ-hydroxyl is engaged in an (i–4) main-chain carbonyl hydrogen bond. Therefore, as with site 130 in the set of buried serine mutants, an (i–4) main-chain hydrogen bond interaction characterizes the most stable buried Thr mutant.

The replacement of the valyl methyl group with a hydroxyl in the buried Val → Thr substitutions is expected to result in a loss of hydrophobic stabilization of about 1.0 kcal/mol. In the case of the Val 149 → Thr mutant, the sequestering of solvent inside the protein reduces the volume of a cavity by 10 Å^3. The corresponding energy of stabilization is, however, modest ($\sim$0.2–0.3 kcal/mol). Therefore the loss of hydrophobic stabilization appears to contribute $\sim$1.0 kcal/mol to the reduction in stability of the buried Val → Thr substitutions.

The "Cost" of Burying a Single Hydroxyl Group. For the solvent-exposed Ala → Ser substitutions the $\Delta\Delta G$ values are all near the helical propensity value of approximately -0.5 kcal/mol (i.e., the mutation destabilizes the protein by approximately 0.5 kcal/mol). To a first approximation this helix-propensity term (among other possible energy terms) is anticipated for all such Ala → Ser substitutions within α-helices, regardless of the solvent accessibility of the site of mutation. Therefore, after adjustment for this value, the $\Delta\Delta G$ contribution for placing the hydroxyl in the core of the protein is approximately -0.5 kcal/mol at site 130, -1.8 kcal/mol at site 42, and -2.0 kcal/mol at site 98. Strain associated with accommodating the additional bulk of the γ-hydroxyl might also contribute to the observed $\Delta\Delta G$ values.

For the Val → Thr mutations the helical propensity difference ($\Delta\Delta G$ value) is expected to be small (~0.1 kcal/mol) (Blaber et al., 1993) and will be ignored.

In general, an Ala → Ser substitution at an internal or congested site might be expected to introduce strain due to steric interference with the wild-type structure. The Val → Thr replacements, however, being essentially isosteric, should mitigate this concern. Nevertheless, the distribution of the $\Delta\Delta G$ values for the Val → Ser substitutions is strikingly similar to that for the Ala → Ser set, even for the buried sites (Figure 13). To a first approximation, therefore, both the Ala → Ser and Val → Thr mutations suggest a range for the thermodynamic cost of the random introduction of a single hydroxyl group in the core region of a protein as 0.5–2.8 kcal/mol. The lowest values within this range correspond to mutants where the side-chain hydroxyl hydrogen bonds with the (i–4) main-chain carbonyl. These results highlight the unique structural relationship between α-helical secondary structure and side chains with γ-hydroxyl groups. An α-helix necessarily provides a potential hydrogen-bonding partner for the side-chain γ-hydroxyl. With regard to threonine, this interaction could not occur if the side-chain methyl and hydroxyl groups were interchanged. One can speculate that this might have been an evolutionary factor in the adoption of the enantiomer of threonine that is found in nature.

In core regions of the protein the potential cost of burying a hydroxyl group is reduced if a hydrogen-bonding partner is available. Substitutions Ala 42 → Ser, Ala 98 → Ser, Val 87 → Thr, and Val 149 → Thr are located within core regions and are within helices, but for reasons previously described, the (i–4) main-chain carbonyl is unavailable as a hydrogen-bonding partner. These mutants must seek alternative hydrogen-bonding partners and therefore better represent the generic introduction of a hydroxyl group into the core region of a protein. In each case, however, it was observed that the hydrogen-bonding potential of the introduced serine or threonine side-chain was at least partially satisfied. It supports previous observations of the importance of satisfying hydrogen bonds in the folded state (Alber et al., 1987). In the extreme case of the Val 149 → Thr substitution, a solvent molecule was sequestered in the protein core. In this case local groups within the protein apparently could not act as satisfactory hydrogen bond partners. Instead, a water molecule was sequestered and served in this role. It suggests that the energy cost of burying a polar group in an environment in which no hydrogen bonding whatsoever is possible could be substantially more than the value of 2.8 kcal/mol observed for Val 149 → Thr.

Related Studies. A number of studies of substitutions including polar/nonpolar replacements at sites within the core region of a protein have been reported (Yutani et al., 1987; Fersht, 1987; Matsumura et al., 1988; Garvey & Matthews, 1989; Stites et al., 1991; Dao-pin et al., 1991; Lim et al., 1992; Shirley et al., 1992; Serrano et al., 1992). The $\Delta\Delta G$ values for Ala → Ser or Val → Thr mutations from these studies vary between –0.8 and –3.2 kcal/mol. This range is very similar to that found here for equivalent substitutions at solvent inaccessible sites. Structural data from other studies are, however, extremely limited, and questions of hydrogen-bonding interactions, local structure, strain, and solvent participation remain unanswered.

The present study does not specifically address the converse type of substitution, Thr → Val and Ala → Ser. At highly solvent-exposed sites Thr → Val and Ala → Ser substitutions are expected to cause changes in energy similar to Val → Thr and Ser → Ala, respectively, but of opposite sign (O'Neil & DeGrado, 1990; Lyu et al., 1990; Blaber et al., 1993). At buried sites the local context is critical. At site 157 in T4 lysozyme, for example, the deletion of a buried hydroxyl destabilizes because a hydrogen-bonding partner is left unsatisfied (Alber et al., 1987). Thus, the same principles that apply to nonpolar → polar substitutions also apply to polar → nonpolar.

Dependence on Solvent Accessibility. The results indicate that the destabilization for randomly chosen Ala → Ser and Val → Thr substitutions is dependent upon the solvent accessibility of the site in question. Figure 13 suggests a general distribution of the mutants into two groups. In one case the side-chain hydroxyl groups are partially solvent-exposed (greater than approximately 15 Å^2) and exhibit a relatively narrow range of $\Delta\Delta G$ values near to the expected helix propensity value. In the other case the side-chain hydroxyl group is essentially solvent-inaccessible (less than 5 Å^2 accessible area), and the $\Delta\Delta G$ values indicate modest to significant destabilization. At the partially accessible sites, even though the solvent-accessible surface is in some cases small, the mutant side-chain apparently can adjust in order to form a hydrogen bond to bulk solvent and so avoid the destabilization that would otherwise be incurred. In order to understand the response of a protein to such substitutions it is critical that not only the structure of the wild-type protein be known but also the mutant structure as well. It could be argued that the overall solvent accessibility of a hydroxyl group, as used in Figure 13, does not take into account the directionality of hydrogen bonding. Therefore we also calculated the solvent-accessible area that would permit hydrogen bonding (i.e., the angle C^β–O^γ–solvent was required to be approximately 120°). This hydrogen-bond accessible solvent area is, in fact, closely proportional to the total solvent-accessible area. Therefore, other than a change of scale, Figure 13 panels a and b are essentially unaffected by the solvent accessible area that is used.

ACKNOWLEDGMENT

The advice and help of Drs. W. A. Baase, L. H. Weaver, D. E. Tronrud, and Ms. J. A. Wozniak are greatly appreciated.

REFERENCES

Alber, T., & Matthews, B. W. (1987) *Methods Enzymol. 154*, 511–533.
Alber, T., Dao-pin, S., Wilson, K., Wozniak, J. A., Cook, S. P., & Matthews, B. W. (1987) *Nature 330*, 41–46.
Bartlett, P. A., & Marlowe, C. K. (1987) *Science 235*, 569–571.
Bash, P. A., Singh, U. C., Brown, F. K., Langridge, R., & Kollman, P. A. (1987) *Science 235*, 574–576.
Becktel, W. J., & Schellman, J. A. (1987) *Biopolymers 26*, 1859–1877.
Blaber, M., Zhang, X.-J., & Matthews, B. W. (1993) *Science 260*, 1637–1640.
Dao-pin, S., Baase, W. A., & Matthews, B. W. (1990) *Proteins 7*, 198–204.
Dao-pin, S., Anderson, D. E., Baase, W. A., Dahlquist, F. W., & Matthews, B. W. (1991) *Biochemistry 30*, 11521–11529.
Eriksson, A. E., Baase, W. A., Zhang, X.-J., Heinz, D. W., Blaber, M., Baldwin, E. P., & Matthews, B. W. (1992) *Science 255*, 178–183.
Fersht, A. R., Shi, J-P., Knill-Jones, J., Lowe, D. M., Wilkinson, A. J., Blow, D. M., Brick, P., Carter, P., Waye, M. M. Y., & Winter, G. (1985) *Nature 314*, 235-238.
Fersht, A. (1987) *Trends Biochem. Sci. 12*, 301–304.
Garvey, E. P., & Matthews, C. R. (1989) *Biochemistry 28*, 2083–2093.

Gray, T. M., & Matthews, B. W. (1984) *J. Mol. Biol. 175*, 75–81.
Green, S. M., Meeker, A. K., & Shortle, D. (1992) *Biochemistry 31*, 5717–5728.
Hamlin, R. (1985) *Methods Enzymol. 114*, 416–452.
Heinz, D. W., Baase, W. A., & Matthews, B. W. (1992) *Proc. Natl. Acad. Sci. U.S.A. 89*, 3751–3755.
Janin, J., Wodak, S., Levitt, M., & Maigret, B. (1978) *J. Mol. Biol. 125*, 357–386.
Jeffrey, G. A., & Saenger, W. (1991) *Hydrogen Bonding in Biological Structures*, Springer-Verlag, Berlin.
Johnson, M. L., & Frasier, S. G. (1985) *Methods Enzymol. 117*, 301–342.
Klotz, I. M., & Franzen, J. S. (1962) *J. Am. Chem. Soc. 84*, 3461–3466.
Kunkel, T. A., Roberts, J. D., & Zakour, R. A. (1987) *Methods Enzymol. 154*, 367–382.
Lee, B., & Richards, F. M. (1970) *J. Mol. Biol. 55*, 379–400.
Lim, W. A., Farruggio, D. C., & Sauer, R. T. (1992) *Biochemistry 31*, 4324–4333.
Lyu, P. C., Liff, M. I., Marky, L. A., & Kallenbach, N. R. (1990) *Science 250*, 669-673.
Marti, T., Otto, H., Mogi, T., Rösselet, S. J., Heyn, M. P., & Khorana, H. G. (1991) *J. Biol. Chem. 266*, 6919–6927.
Matsumura, M., & Matthews, B. W. (1989) *Science 243*, 792–794.
Matsumura, M., Becktel, W. J., & Matthews, B. W. (1988) *Nature 334*, 406–410.
Muchmore, D. C., McIntosh, L. P., Russell, C. B., Anderson, D. E., & Dahlquist, F. W. (1989) *Methods Enzymol. 177*, 44–73.
O'Neil, K. T., & DeGrado, W. F. (1990) *Science 250*, 646–651.
Pauling, L. (1960) *The Nature of the Chemical Bond*, third ed., Cornell University Press.
Poteete, A. R., Dao-pin, S., Nicholson, H., & Matthews, B. W. (1991) *Biochemistry 30*, 1425–1432.
Remington, S. J., Anderson, W. F., Owen, J., Ten Eyck, L. F., Grainger, C. T., & Matthews, B. W. (1978) *J. Mol. Biol. 118*, 81–98.
Richardson, J. S., & Richardson, D. C. (1988) *Science 240*, 1648–1652.
Roseman, M. A. (1988a) *J. Mol. Biol. 200*, 513–522.
Roseman, M. A. (1988b) *J. Mol. Biol. 201*, 621–623.
Rossmann, M. G. (1979) *J. Appl. Crystallogr. 12*, 225–239.
Schmid, M. F., Weaver, L. H., Holmes, M. A., Grütter, M. G., Ohlendorf, D. H., Reynolds, R. A., Remington, S. J., & Matthews, B. W. (1981) *Acta Crystallogr. A37*, 701–710.
Serrano, L., Kellis, J. T., Jr., Cann, P., Matouschek, A., & Fersht, A. R. (1992) *J. Mol. Biol. 224*, 783–804.
Shirley, B. A., Stanssens, P., Hahn, U., & Pace, C. N. (1992) *Biochemistry 31*, 725-732.
Sneddon, S. F., Tobias, D. J., & Brooks, C. L., III (1989) *J. Mol. Biol. 209*, 817–820.
Stites, W. E., Gittis, A. G., Lattman, E. E., & Shortle, D. (1991) *J. Mol. Biol. 221*, 7-14.
Sundaralingam, M., & Sekharudu, Y. C. (1989) *Science 244*, 1333–1337.
Tronrud, D. E. (1992) *Acta Crystallogr. A48*, 912–916.
Tronrud, D. E., Ten Eyck, L. F., & Matthews, B. W. (1987) *Acta Crystallogr. A43*, 489–503.
Weaver, L. H., & Matthews, B. W. (1987) *J. Mol. Biol. 193*, 189–199.
Yutani, K., Ogasahara, K., Tsujita, T., & Sugino, Y. (1987) *Proc. Natl. Acad. Sci. U.S.A. 84*, 4441–4444.
Zhang, X.-J., Baase, W. A., & Matthews, B. W. (1991) *Biochemistry 30*, 2012–2017.